Synthesis and characterization of copper-manganese ferrites with composition Cu$_{1-x}$Mn$_x$Fe$_2$O$_4$ supported on activated carbon

T. M. Petrova[1]*, N. I. Velinov[1], I. G. Genova[2], T. S. Tsoncheva[2],
D. G. Kovacheva[3], N. V. Petrov[2], I. G. Mitov[1]

[1] *Institute of Catalysis, Bulgarian Academy of Sciences, Acad. G. Bonchev str., bl. 11, 1113 Sofia, Bulgaria*
[2] *Institute of Organic Chemistry with Centre of Phytochemistry, Bulgarian Academy of Sciences, Acad. G. Bonchev str., bl. 9, 1113 Sofia, Bulgaria*
[3] *Institute of General and Inorganic Chemistry, Bulgarian Academy of Sciences, Acad. G. Bonchev str., bl. 11, 1113 Sofia, Bulgaria*

The present study is addressed to the synthesis of mixed copper-manganese ferrite catalysts Cu$_{1-x}$Mn$_x$Fe$_2$O$_4$ (x=0; 0.2; 0.4; 0.6; 0.8; 1) supported on activated carbon from peach stones. The samples were characterized by X-ray diffraction, Mössbauer spectroscopy and methanol decomposition to CO and hydrogen was used as a catalytic test. The formation of ferrite catalysts with cubic and partially inverse spinel structure was established. Significant changes under the reaction medium of the ferrite materials with the formation of magnetite and carbide of Haag were registered. The presence of copper in the manganese ferrites improves the catalytic activity at the low-temperature and this tendency increases with the increase of copper content.

Keywords: copper-manganese ferrites, activated carbon, Mössbauer spectroscopy, methanol decomposition.

INTRODUCTION

Ferrite materials are attractive area for intensive research due to their wide application in electronics [2], catalysis [3], biology and medicine [4], etc. Depending on the location of the cations in the crystal lattice the spinel type ferrites are classified in three main groups: normal, inverse and partially inverse. In the normal spinels all two-valent cations are located only on tetrahedral positions, while in the inverse spinels all two-valent cations occupy only octahedral positions and in the partially inverse spinels, the two-valent cations are located partially at tetrahedral and octahedral positions. It is well-known that various metallic ions may preferably occupy various coordination positions [5]. Moreover, the distribution of the ions in the structure of the spinel affects both the physical and catalytic features [6, 7]. Spinel ferrites are effective catalysts for photo-splitting of methanol/water solution [8], methane reforming [9], steam reforming of methanol and ethanol [10, 11] and methanol decomposition [12–17]. It has been established, that mixed ferrites such as Cu$_{1-x}$Co$_x$Fe$_2$O$_4$ and Cu$_{1-x}$Zn$_x$Fe$_2$O$_4$ exhibit better catalytic activity in methanol decomposition than the mono-component ones [13, 14], [16], [18, 19]. In the recent years the activated carbons based on low-cost agricultural wastes are widely used as adsorbents and supports for catalysts due to their textural characteristics, surface functionality and stability which could be easily controlled during the process of the pyrolysis and carbon treatment [20–24]. Iron modified activated carbon from various agriculture wastes were tested as catalysts in methanol decomposition in ref. [20]. During the reaction the larger particles easily transformed to Fe and/or Fe$_3$C that resulted in low catalytic activity and high selectivity to CO [20]. The predominant effect of the surface functionality over the texture characteristics of the activated carbon on the state of loaded iron phase was discussed. The aim of the present investigation is synthesis and characterization of supported on activated carbon from peach stones mixed copper-manganese ferrite catalysts with different composition. Their behaviour as catalysts in methanol decomposition is also in the focus of the study.

---

* To whom all correspondence should be sent:
e- mail: silberbarren@abv.bg

EXPERIMENTAL

Synthesis

Activated carbon support was obtained by pyrolysis of waste peach stones at 550°C (heating rate of 5°C/min) at atmospheric pressure and further activation with water vapor at 800°C for 1 h. The activated carbon was impregnated by aqueous solution of $Cu(NO_3)_2 \cdot 3H_2O$, $Mn(NO_3)_2 \cdot 4H_2O$ and $Fe(NO_3)_3 \cdot 9H_2O$ using ultrasonic treatment on a BANDELIN SONOPULS HD 2200. The samples were dried at 50°C for 24 hours and then heated at 500°C for 2 hours in a nitrogen atmosphere. The obtained materials contained 8 wt% metal are denoted as $Cu_{1-x}Mn_xFe_2O_4$/ACP, where x=0; 0.2; 0.4; 0.6; 0.8 and 1.

Methods of characterization

Powder X-ray diffraction (XRD) patterns were collected within the range of 10° to 80° 2θ on a Bruker D8 Advance diffractometer with Cu K_α radiation and LynxEye detector. Phase identification was performed using ICDD-PDF2 Database. The average crystallites size (D), the degree of microstrain (e) and the lattice parameters (a) of the studied ferrites were determined from the experimental XRD profiles by using the PowderCell-2.4 software and appropriate corrections for the instrumental broadening.

The Mössbauer spectra were obtained in air at room temperature (RT) with a Wissel (Wissenschaftliche Elektronik GmbH, Germany) electromechanical spectrometer working in a constant acceleration mode. A ^{57}Co/Rh (activity $\cong$ 50 mCi) source and α-Fe standard were used. The experimentally obtained spectra were fitted using CONFIT2000 software [25]. The parameters of hyperfine interaction such as isomer shift (δ), quadrupole splitting (ΔE_q), effective internal magnetic field (B), line widths (Γ_{exp}), and relative weight (G) of the partial components in the spectra were determined.

Catalytic experiments

Methanol conversion was carried out in a fixed bed flow reactor (0.055 g of catalyst), argon being used as a carrier gas (50 cm³ min⁻¹). The methanol partial pressure was 1.57 kPa. The catalysts were tested under conditions of a temperature-programmed regime within the range of 80–500°C with heating rate of 1°C.min⁻¹. On-line gas chromatographic analyses were performed on HP apparatus equipped with flame ionization and thermoconductivity detectors, on a PLOT Q column, using an absolute calibration method and a carbon based material balance.

RESULTS AND DISCUSSION

The X-Ray diffraction patterns are presented in Figure 1 and the corresponding data are listed in Table 1. Diffraction maxima of cubic spinel phase (S.G. Fd-3m) are observed in all spectra. In addition diffractions of small quantities of CuO (PDF 80-1917), Cu_2O (PDF 78-2076) and Cu (PDF 4-0836) are also registered. The increase of Mn content in binary ferrites leads to the increase in the lattice parameter, which was 8.34 Å and 8.45 Å for $CuFe_2O_4$ and $MnFe_2O_4$, respectively. This is probably due to the larger ionic radius of Mn^{2+} than this of Cu^{2+}. According to [26] the crystal radius in octahedral coordination of Mn^{2+} is 0.97 Å, while that of Cu^{2+} is 0.87 Å. No linear dependence of the average crystallite size of ferrites on their composition is observed. The largest crystallite size, which was detected for $Cu_{0.5}Mn_{0.5}Fe_2O_4$/ACP could be attributed to the inhomogeneous surface of the activated carbon, which probably reflects on the mechanisms of the formation of the primary microcrystals. There are no simple relation between the spinel composition and microstrain degrees.
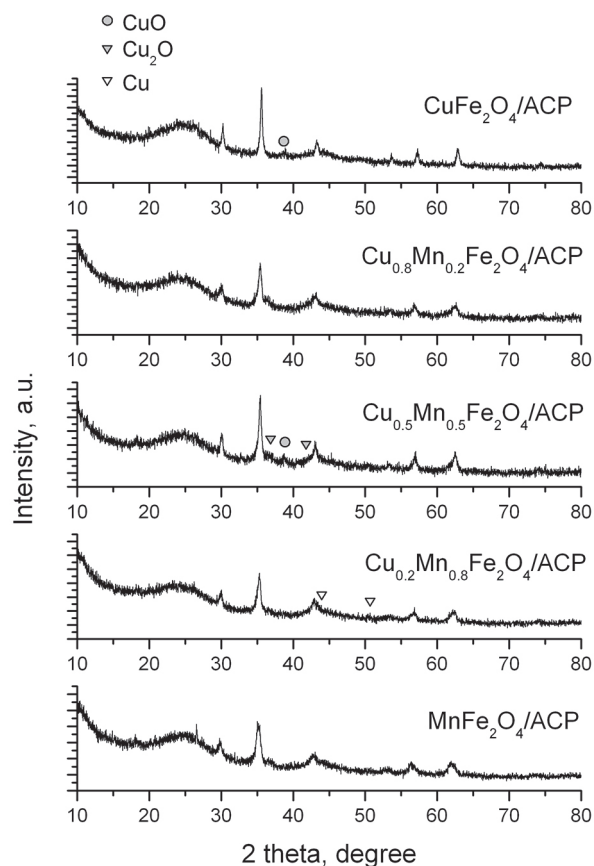

Fig. 1. X-ray diffraction patterns of samples of $Cu_{1-x}Mn_xFe_2O_4$ supported on activated carbon thermally treated at 500°C.

Table 1. Average crystallites size (D), degree of microstrain (e) and lattice parameter (a) of the ferrite phase in samples treated at 500°C determined from the experimental XRD profiles

Sample	Phase	D, nm	$e_* 10^3$, a.u.	a, Å	Additional phases
$CuFe_2O_4$ /ACP	Spinel	18.79	2.14	8.34	CuO
$Cu_{0.8}Mn_{0.2}Fe_2O_4$ /ACP	Spinel	19.83	5.17	8.41	–
$Cu_{0.5}Mn_{0.5}Fe_2O_4$ /ACP	Spinel	47.27	5.07	8.40	CuO, Cu_2O
$Cu_{0.2}Mn_{0.8}Fe_2O_4$ /ACP	Spinel	22.58	2.05	8.43	Cu
$MnFe_2O_4$/ACP	Spinel	17.65	6.67	8.45	–

The Mössbauer spectra of samples obtained after drying are shown in Figure 2 and the calculated parameters of the spectra are presented in Table 2. All of the spectra are quadrupole doublets which parameters are typical of Fe^{3+} in octahedral coordination. The experimental spectra of the samples after thermal treatment at 500°C (Figure 3, Table 3) are well fitted with a model of three sextets and one doublet. The sextet (Sx1) corresponds to iron in tetrahedral position and the two sextets (Sx2 and Sx3), for iron in octahedral coordination. The sextet with higher values of magnetic field (Sx2) is due to stronger magnetic interactions between iron ions, which have smaller number non-magnetic neighbor ions (Cu^{2+}, Mn^{2+}), while the sextet with lower magnetic field (Sx3) corresponds to iron ions with more copper and manganese neighbors ions. It was observed increased isomer shift of the sextet components of iron in octahedral positions for the mixed copper-manganese ferrite. This indicates the presence of mixed-valence iron in octahedral coordination. The presence of a doublet component could be due to the presence of paramagnetic component, formed by iron ions located in the medium of hydrocarbon functional groups from the activated carbon surface. Alternatively, this component could be due to pres-
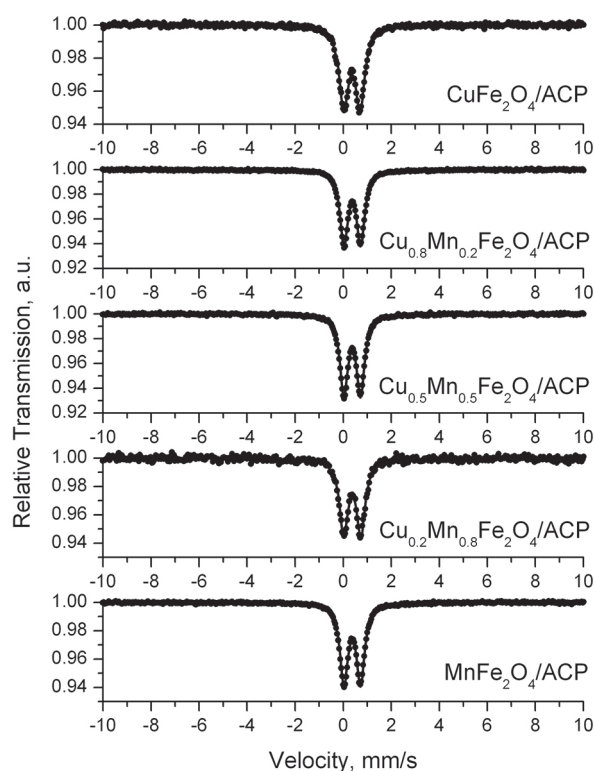

Fig. 2. Mössbauer spectra of samples of $Cu_{1-x}Mn_xFe_2O_4$ supported on activated carbon after drying at 50°C.
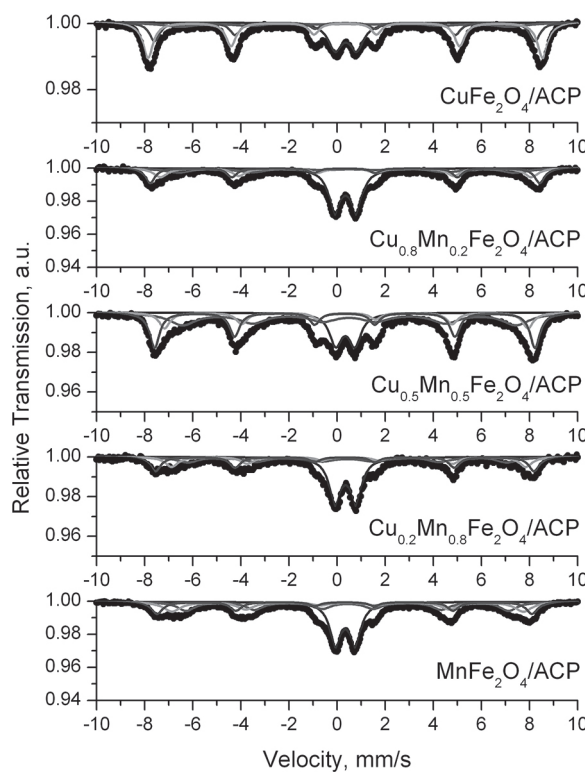

Fig. 3. Room temperature Mössbauer spectra of samples of $Cu_{1-x}Mn_xFe_2O_4$ supported on activated carbon thermally treated at 500°C.

Table 2. Mössbauer parameters of samples of $Cu_{1-x}Mn_xFe_2O_4$ supported on activated carbon after drying at 50°C (δ – isomer shift, ΔE_q – quadrupole splitting, B – effective internal magnetic field, Γ_{exp} – line widths, G – relative weight of the partial components in the spectra)

Sample	Components	δ, mm/s	ΔE_q, mm/s	B, T	Γ_{exp}, mm/s	G, %
$CuFe_2O_4$/ACP	Db-Fe^{3+}	0.36	0.68	–	0.46	100
$Cu_{0.8}Mn_{0.2}Fe_2O_4$/ACP	Db-Fe^{3+}	0.38	0.70	–	0.40	100
$Cu_{0.5}Mn_{0.5}Fe_2O_4$/ACP	Db-Fe^{3+}	0.38	0.70	–	0.39	100
$Cu_{0.2}Mn_{0.8}Fe_2O_4$/ACP	Db-Fe^{3+}	0.38	0.72	–	0.43	100
$MnFe_2O_4$/ACP	Db-Fe^{3+}	0.38	0.70	–	0.40	100

Table 3. Mössbauer parameters of samples of $Cu_{1-x}Mn_xFe_2O_4$ supported on activated carbon thermally treated at 500°C (δ – isomer shift, ΔE_q – quadrupole splitting, B – effective internal magnetic field, Γ_{exp} – line widths, G – relative weight of the partial components in the spectra, LNT – spectra measured at liquid nitrogen temperature)

Sample	Components	δ, mm/s	ΔE_q, mm/s	B, T	Γ_{exp}, mm/s	G, %
$CuFe_2O_4$/ACP	Sx1- Fe-tetra	0.33	−0.01	49.2	0.51	22
	Sx2- Fe-octa	0.34	0.00	51.0	0.52	41
	Sx3- Fe-octa	0.33	−0.02	42.6	1.74	16
	Db-Fe^{3+}	0.37	0.89	–	0.71	21
$Cu_{0.8}Mn_{0.2}Fe_2O_4$/ACP	Sx1- Fe-tetra	0.32	0.00	50.3	0.50	21
	Sx2- Fe-octa	0.38	−0.02	47.9	0.68	21
	Sx3- Fe-octa	0.45	−0.10	43.1	1.53	21
	Db-Fe^{3+}	0.35	0.88	–	0.62	37
$Cu_{0.5}Mn_{0.5}Fe_2O_4$/ACP	Sx1- Fe-tetra	0.32	0.00	49.2	0.50	31
	Sx2- Fe-octa	0.39	−0.03	47.0	0.54	16
	Sx3- Fe-octa	0.51	0.01	43.1	1.37	36
	Db-Fe^{3+}	0.34	0.80	–	0.62	17
$Cu_{0.2}Mn_{0.8}Fe_2O_4$/ACP	Sx1- Fe-tetra	0.32	0.00	48.9	0.53	23
	Sx2- Fe-octa	0.51	−0.05	45.7	0.63	18
	Sx3- Fe-octa	0.43	0.00	41.0	1.15	22
	Db-Fe^{3+}	0.35	0.86	–	0.59	37
$MnFe_2O_4$/ACP	Sx1- Fe-tetra	0.31	0.00	48.4	0.57	19
	Sx2- Fe-octa	0.44	0.01	45.4	0.85	23
	Sx3- Fe-octa	0.44	−0.02	41.7	0.85	26
	Db-Fe^{3+}	0.34	0.82	–	0.57	32
$Cu_{0.8}Mn_{0.2}Fe_2O_4$/ACP-LNT	Sx1- Fe-tetra	0.44	0.00	51.5	0.39	21
	Sx2- Fe-octa	0.47	0.03	53.0	0.35	15
	Sx3- Fe-octa	0.46	−0.09	49.4	0.95	27
	Db-Fe^{3+}	0.45	0.93	–	0.56	37
$Cu_{0.2}Mn_{0.8}Fe_2O_4$/ACP-LNT	Sx1- Fe-tetra	0.45	0.00	51.2	0.41	24
	Sx2- Fe-octa	0.47	0.02	52.7	0.36	14
	Sx3- Fe-octa	0.52	−0.11	49.0	0.98	28
	Db-Fe^{3+}	0.45	0.92	–	0.55	34
$MnFe_2O_4$/ACP-LNT	Sx1- Fe-tetra	0.45	0.00	51.0	0.39	22
	Sx2- Fe-octa	0.48	0.04	52.4	0.42	24
	Sx3- Fe-octa	0.51	−0.10	49.2	0.72	25
	Db-Fe^{3+}	0.45	0.86	–	0.56	29

ence of particles exhibiting superparamagnetic behaviour at room temperature. This supposition was supported by the Mössbauer spectra of the samples at the temperature of liquid nitrogen (Figure 4 and Table 3), where no significant changes with the doublet part of the spectra were detected.

The temperature dependencies of methanol decomposition on various ferrite materials are pre-
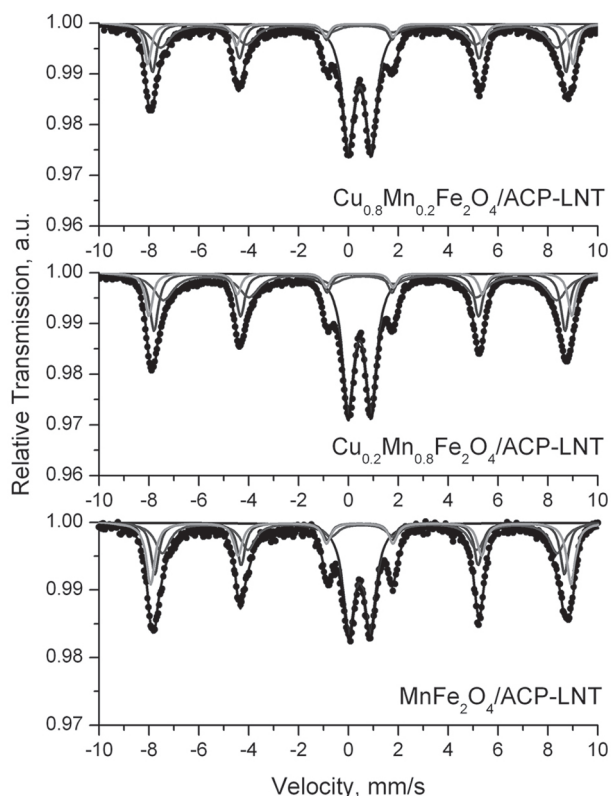
Fig. 4. Liquid nitrogen temperature Mössbauer spectra of samples of $Cu_{1-x}Mn_xFe_2O_4$ supported on activated carbon thermally treated at 500°C.

sented in Figure 5a. The selectivity to CO, which formation is directly related to the ability of catalysts to release hydrogen, is shown in Figure 5b. Methane (up to 26%) and CO_2 (up to 27%) are also registered as by-products. $MnFe_2O_4$/ACP sample exhibits catalytic activity just above 340°C and 80% conversion is achieved at 440°C. All copper containing materials demonstrate catalytic activity at about 100–150°C lower temperature. Among them, $CuFe_2O_4$/ACP possesses the lowest catalytic activity and well defined tendency of deactivation above 410°C. The catalytic activity of binary materials is higher than the mono component ones and this feature is most pronounced with the increase of copper content in them. Note the specific course of the temperature dependencies for all $Cu_{1-x}Mn_xFe_2O_4$ mixed ferrites. They all characterise with a slope at 260–350°C and a steep increase in the catalytic activity above it.

The Mössbauer data of the samples after the catalytic test are presented in Figure 6 and Table 4. All spectra of samples after test are changed in different degree. The best fitting of $CuFe_2O_4$/ACP, $Cu_{0.5}Mn_{0.5}Fe_2O_4$/ACP and $Cu_{0.2}Mn_{0.8}Fe_2O_4$/ACP spectra after test was done using a model consists of two sextets and one doublet. The absence of the third sextet in spectra of these samples after catalysis could be explain with partial reduction of Cu^{2+} to
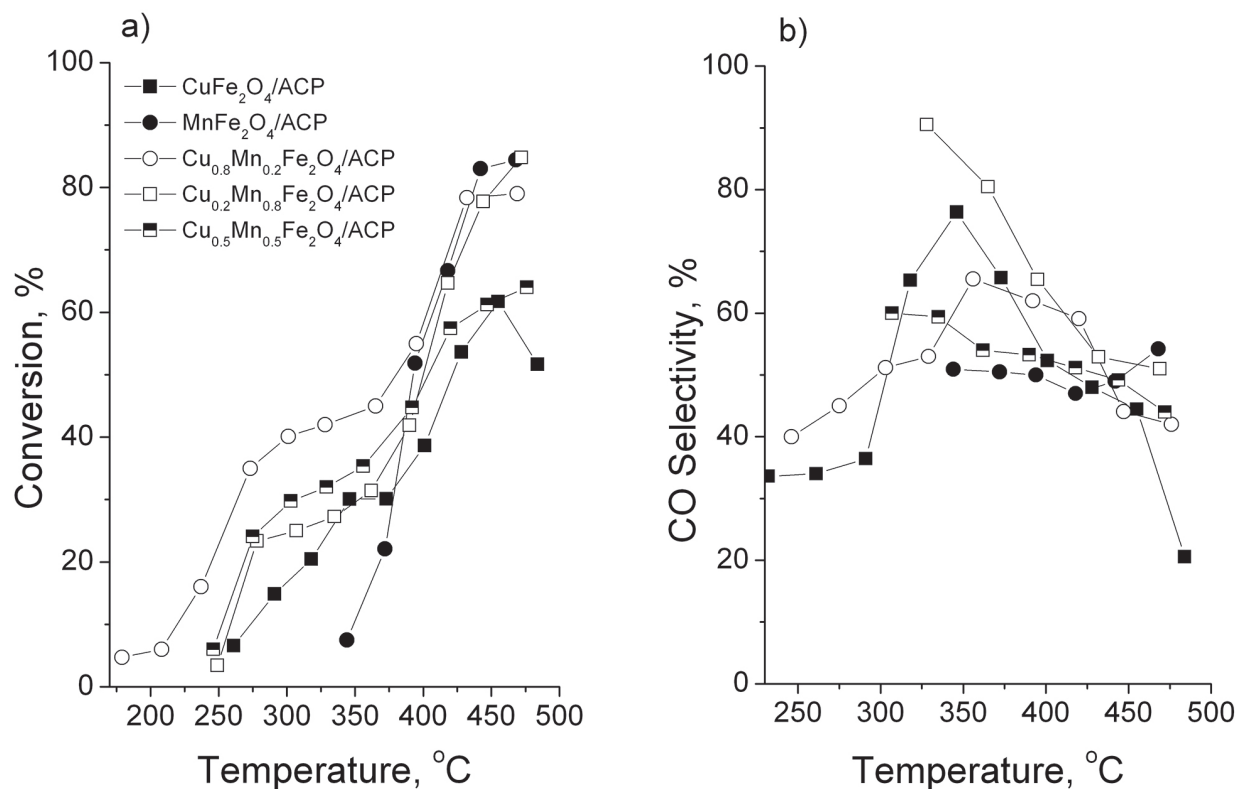

Fig. 5. Temperature dependencies of conversion (a) and CO selectivity (b) in methanol decomposition of thermally treated at 500°C samples.

Table 4. Mössbauer parameters of samples of $Cu_{1-x}Mn_xFe_2O_4$ supported on activated carbon after methanol decomposition test (δ – isomer shift, ΔE_q – quadrupole splitting, B – effective internal magnetic field, Γ_{exp} – line widths, G – relative weight of the partial components in the spectra)

Sample	Components	δ, mm/s	ΔE_q, mm/s	B, T	Γ_{exp}, mm/s	G, %
$CuFe_2O_4$/ACP-MD	Sx1-Fe-tetra	0.34	0.00	49.9	0.50	31
	Sx2-Fe-octa	0.38	−0.02	47.1	1.66	38
	Db1-Fe^{3+}	0.35	0.86	–	0.92	31
$Cu_{0.8}Mn_{0.2}Fe_2O_4$/ACP-MD	Sx1-χ-Fe_5C_2	0.19	0.06	20.6	0.45	37
	Sx2-χ-Fe_5C_2	0.15	0.07	18.5	0.33	12
	Sx3-χ-Fe_5C_2	0.26	0.09	10.9	0.35	3
	Db1-Fe^{3+}	0.34	0.83	–	0.62	48
$Cu_{0.5}Mn_{0.5}Fe_2O_4$/ACP-MD	Sx1-Fe-tetra	0.33	0.00	49.3	0.50	31
	Sx2-Fe-octa	0.48	0.05	45.5	1.17	40
	Db1-Fe^{3+}	0.35	0.76	–	0.71	29
$Cu_{0.2}Mn_{0.8}Fe_2O_4$/ACP-MD	Sx1-Fe-tetra	0.31	0.00	49.3	0.48	23
	Sx2-Fe-octa	0.58	0.03	45.4	1.02	26
	Db1-Fe^{3+}	0.32	0.78	–	0.64	51
$MnFe_2O_4$/ACP-MD	Sx1-χ-Fe_5C_2	0.19	0.05	21.1	0.38	35
	Sx2-χ-Fe_5C_2	0.17	0.03	19.5	0.36	12
	Sx3-χ-Fe_5C_2	0.23	0.00	11.0	0.35	3
	Db1-Fe^{3+}	0.35	0.77	–	0.56	50

Cu^0 and therefore decrease of number of octahedral iron with non-iron neighbors. The spectra of $Cu_{0.8}Mn_{0.2}Fe_2O_4$/ACP and $MnFe_2O_4$/ACP after catalysis are changed significantly and are well fitted

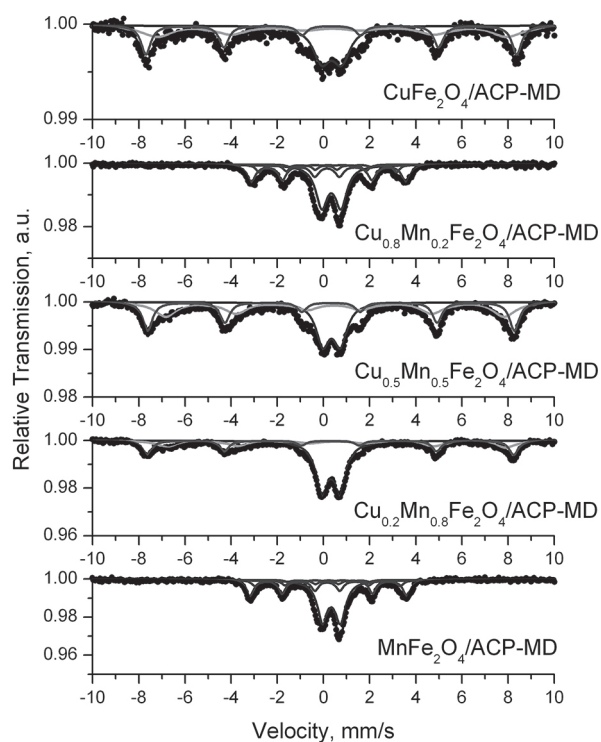**Fig. 6.** Mössbauer spectra of samples of $Cu_{1-x}Mn_xFe_2O_4$ supported on activated carbon after methanol decomposition test.

with a model including three sextets and one doublet. The calculated parameters of the sextets correspond to carbide of Haag (χ-Fe_5C_2). In all spectra of the samples after catalytic test are present doublets corresponding to Fe^{3+} ions with similar parameters to doublets in the spectra of the samples before test, but with higher relative weight. This suggest that doublets correspond to an unchanged during reaction phase or due to a new one with high content of non- iron ions. The comparison of these Mössbauer results with the catalytic data clearly indicate that the reduction changes with the ferrites under the reaction medium leads to their complex catalytic behaviour. The high catalytic activity for all binary samples at lower temperature seems to be facilitated by the copper ions in the vicinity of manganese ones, which is realized in the ferrite structure. However at higher temperatures the catalytic behaviour is probably promoted by the activity of Mn^{2+}-Fe^{3+} couples and the formation of carbide phase during the reaction, as well.

CONCLUSIONS

Copper-manganese ferrite catalysts $Cu_{1-x}Mn_xFe_2O_4$ supported on activated carbon was synthesized. The formation of cubic spinel ferrite with partial inverse structure was established. Binary ferrites possess higher catalytic activity at lower temperature in comparison with their mono-component analogues. They are significantly change under the reaction medium and at higher temperatures the catalytic

behaviour is probably promoted by the activity of Mn^{2+}-Fe^{3+} couples and the formation of carbide phase.

REFERENCES

1. M. N. Ashiq, F. Naz, M. A. Malana, R. S. Gohar, Z. Ahmad, *Mater. Res. Bull*., **47**, 683 (2012).
2. K. Mukherjee, S. B. Majumder, *Sensor Actuator B-Chem*, **162**, 229 (2012).
3. R. Benrabaa, H. Boukhlouf, S. Barama, E. Bordes-Richard, R. N. Vannier, A. Barama, *Catal. Lett*., **142**, 42 (2012).
4. K. E. Scarberry, E. B. Dickerson, Z. J. Zhang, B. B. Benigno, J. F. McDonald, *Nanomed-Nanotechnol*, **6**, 399 (2010).
5. P. V. Kovtunenko, *Glass Ceram*., **54**, 143 (1997).
6. T. A .S. Ferreira, J. C. Waerenborgh, M. H. R. M. Mendoca, M. R. Nunes, F. M. Costa, *Solid State Sci.*, **5**, 383 (2003).
7. J.-P. Jacobs, A. Maltha, J. G. H. Reintjes, J. Drimal, V. Ponec, H. H. Brongersma, *J. Catal*., **147**, 294 (1994).
8. H. S. Kim, D. Kim, B. S. Kwak, G. B. Han, M.-H. Um, M. Kang, *Chem. Eng. J*., **243**, 272 (2014).
9. R. Benrabaa, H. Boukhlouf, A. Löfberg, A. Rubbens, R.-N. Vannier, E. B.-Richard, A. Barama, *J. Nat. Gas Chem.*, **21**, 595 (2012).
10. Y.-H. Huang, S.-F. Wang, A.-P. Tsai, S. Kameoka, *Ceram. Int.*, **40**, 4541 (2014).
11. S. Hull, J. Trawczyński, *Int. J. Hydrog. Energy*, **39**, 4259 (2014).
12. E. Manova, T. Tsoncheva, C. Estournes, D. Paneva, K. Tenchev, I. Mitov, L. Petrov, *Appl. Catal. A Gen*., **300**, 170 (2006).
13. N. Velinov, K. Koleva, T. Tsoncheva, D. Paneva, E. Manova, K. Tenchev, B. Kunev, I. Genova, I. Mitov, *Cent. Eur. J. Chem*., **12**, 250 (2014).
14. N. Velinov, K. Koleva, T. Tsoncheva, E. Manova, D. Paneva, K. Tenchev, B. Kunev, I. Mitov, *Catal. Commun*., **32**, 41 (2013).
15. N. Velinov, E. Manova, T. Tsoncheva, C. Estournès, D. Paneva, K. Tenchev, V. Petkova, K. Koleva, B. Kunev, I. Mitov, *Solid State Sci*., **14**, 1092 (2012).
16. T. Tsoncheva, E. Manova, N. Velinov, D. Paneva, M. Popova, B. Kunev, K. Tenchev, I. Mitov, *Catal. Commun*., **12**, 105 (2010).
17. E. Manova, T. Tsoncheva, D. Paneva, I. Mitov, K. Tenchev, L. Petrov, *Appl. Catal. A Gen*., **277**, 119 (2004).
18. K. Koleva, N. Velinov, T. Tsoncheva, I. Mitov, *Hyperfine Interact*., **226**, 89 (2014).
19. K. Koleva, N. Velinov, T. Tsoncheva, I. Mitov, B. Kunev, *Bulg. Chem. Commun.*, **45(4)**, 434 (2013).
20. T. Tsoncheva, N. Velinov, R. Ivanova, I. Stoycheva, B. Tsyntsarski, I. Spassova, D. Paneva, G. Issa, D. Kovacheva, I. Genova, I. Mitov, N. Petrov, *Microporous and Mesoporous Materials*, **217**, 87 (2015).
21. F. Rodriguez-Reinoso, *Carbon*, **36**, 159, (1998).
22. H. Juntgen, *Fuel*, **65**, 1436 (1986).
23. C. Moreno-Castilla, F. Carrasco-Marin, C. Parejo-Perez, M. V. Lopez Ramon, *Carbon*, **39**, 869 (2001).
24. F. Rodriguez-Reinoso, M. Molina-Sabio, M. A. Munecas, *J. Phys. Chem*., **96**, 2707 (1992).
25. T. Žák, Y. Jirásková, *Surf. Interface Anal*., **38**, 710 (2006).
26. R. D. Shannon, *Acta Cryst.*, **A 32**, 751 (1976).

СИНТЕЗ И ОХАРАКТЕРИЗИРАНЕ НА МЕД-МАНГАНОВИ ФЕРИТИ СЪС СЪСТАВ $Cu_{1-x}Mn_xFe_2O_4$, НАНЕСЕНИ ВЪРХУ АКТИВЕН ВЪГЛЕН

Т. М. Петрова[1]*, Н. И. Велинов[1], И. Г. Генова[2], Т. С. Цончева[2],
Д. Г. Ковачева[3], Н. В. Петров[2], И. Г. Митов[1]

[1] *Институт по катализ, Българска академия на науките, 1113, София, България*
[2] *Институт по органична химия с център по фитохимия, Българска академия на науките,*
1113, София, България
[3] *Институт по обща и неорганична химия, Българска академия на науките,*
1113 София, България

(Резюме)

Целта на настоящото проучване е да се синтезират смесено оксидни мед манганови феритни катализатори със състав $Cu_{1-x}Mn_xFe_2O_4$ (x=0; 0.2; 0.4; 0.6; 0.8 and 1), нанесени върху активен въглен, получен от костилки от праскови. За охарактеризиране структурата и катийонното разпределение на синтезираните образци са използвани Рентгенова дифракция, Мьосбауерова спектроскопия и е проведен каталитичен тест в реакция на разлагане на метанол. Резултатите от анализите дават доказателства, че са получени нанесени феритни катализатори с кубична симетрия и частично инверсна шпинелна структура. Установи се, че катализаторите претърпяват съществени редукционни промени с формиране на магнетит или карбид на Хааг под действието на реакционната среда. Доказа се, че присъствието на мед в манагановите ферити подобрява каталитичната активност в нискотемпературната област като тази тенденция нараства с повишаване съдържанието на мед в образците.